Radiative Sensitivity to Water Vapor under All-Sky Conditions

JOHN FASULLO

Program in Atmospheric and Oceanic Sciences, University of Colorado, Boulder, Colorado

DE-ZHENG SUN

Climate Diagnostics Center, NOAA–CIRES, University of Colorado, Boulder, Colorado

2 October 2000

ABSTRACT

Using the National Center for Atmospheric Research Community Climate Model, version 3, radiation transfer model and a realistic tropospheric environment including the International Satellite Cloud Climatology Project cloud fields, all-sky radiative sensitivity to water vapor is assessed. The analysis improves upon previous clear-sky and model-based studies by using observed clouds, assessing realistic vertically varying perturbations, and considering spatial gradients in sensitivity through the Tropics and subtropics. The linearity of sensitivity is also explored. The dry zones of the subtropics and the eastern Pacific Ocean are found to be particularly sensitive to the water vapor distribution, especially for variations in the upper troposphere. The cloud field is instrumental in determining spatial gradients in sensitivity both at the top of the atmosphere and the surface. Throughout the Tropics, outgoing longwave radiation is most sensitive to water vapor in the upper troposphere, especially when perturbations characteristic of either natural variations or measurement uncertainties are considered. In contrast, surface radiative fluxes are everywhere most sensitive to specific humidity variations in the lower troposphere.

1. Introduction

The radiative effects of water vapor constitute a major thermal forcing of the climate system (Manabe and Wetherald 1967; Lindzen 1990; Betts 1990; Rind et al. 1991; Sun and Lindzen 1993a,b; Sun and Oort 1995; Sun and Held 1996; Schneider et al. 1999). Considerable uncertainty exists, however, in even the mean water vapor distribution as revealed by the large differences among existing ''datasets'' of water vapor. Figure 1a displays the longitude–height humidity difference between reanalyzed estimates from the National Centers for Environmental Prediction–National Center for Atmospheric Research (NCEP–NCAR; Kalnay et al. 1996) and the European Centre for Medium-Range Weather Forecasts (ECMWF; Gibson et al. 1997) from 1979 to 1993. Though the reanalyses differ in their details, the NCEP–NCAR fields are generally moister than the ECMWF fields, with differences near 10% in the lower troposphere and over 25% in much of the upper troposphere. In Fig. 1b, a plan view comparison between total precipitable water from 500 to 300 mb is shown based on the ECMWF reanalysis and the National Aeronautics and Space Administration Water Vapor Project (NVAP; Randel et al. 1996) from 1988 to 1992. Differences between ECMWF and NVAP fields are not significantly smaller than between the reanalyses as they exceed 25% through much of the Indian and eastern Pacific Oceans. It is known that, in part, differences between the various datasets stem from the error present in the radiosonde record (e.g., Elliot and Gaffen 1991; Zipser and Johnson 1998).

Radiative sensitivity to water vapor therefore needs to be assessed in order to estimate the impact of uncertainties in the water vapor distribution on model simulations. Shine and Sinha (1991) examine the sensitivity of three idealized and cloudless atmospheric profiles to vertically discrete water vapor perturbations. Peak sensitivity is found for perturbations near 800 mb. Schneider et al. (1999) examine the sensitivity of climate to water vapor in a coupled model under a carbon dioxide doubling with prescribed model clouds. In contrast to Shine and Sinha, they find peak sensitivity at the top of the atmosphere (TOA) for water vapor changes near 500 mb. The sensitivity of radiative fluxes to vertically varying water vapor variations in an atmosphere with observed clouds has yet to be established, however.

A numeric simulation of the atmosphere's radiative

Corresponding author address: Dr. John Fasullo, PAOS, University of Colorado, CB 311, Boulder, CO 80309–0311.
E-mail: john.fasullo@colorado.edu

© 2001 American Meteorological Society

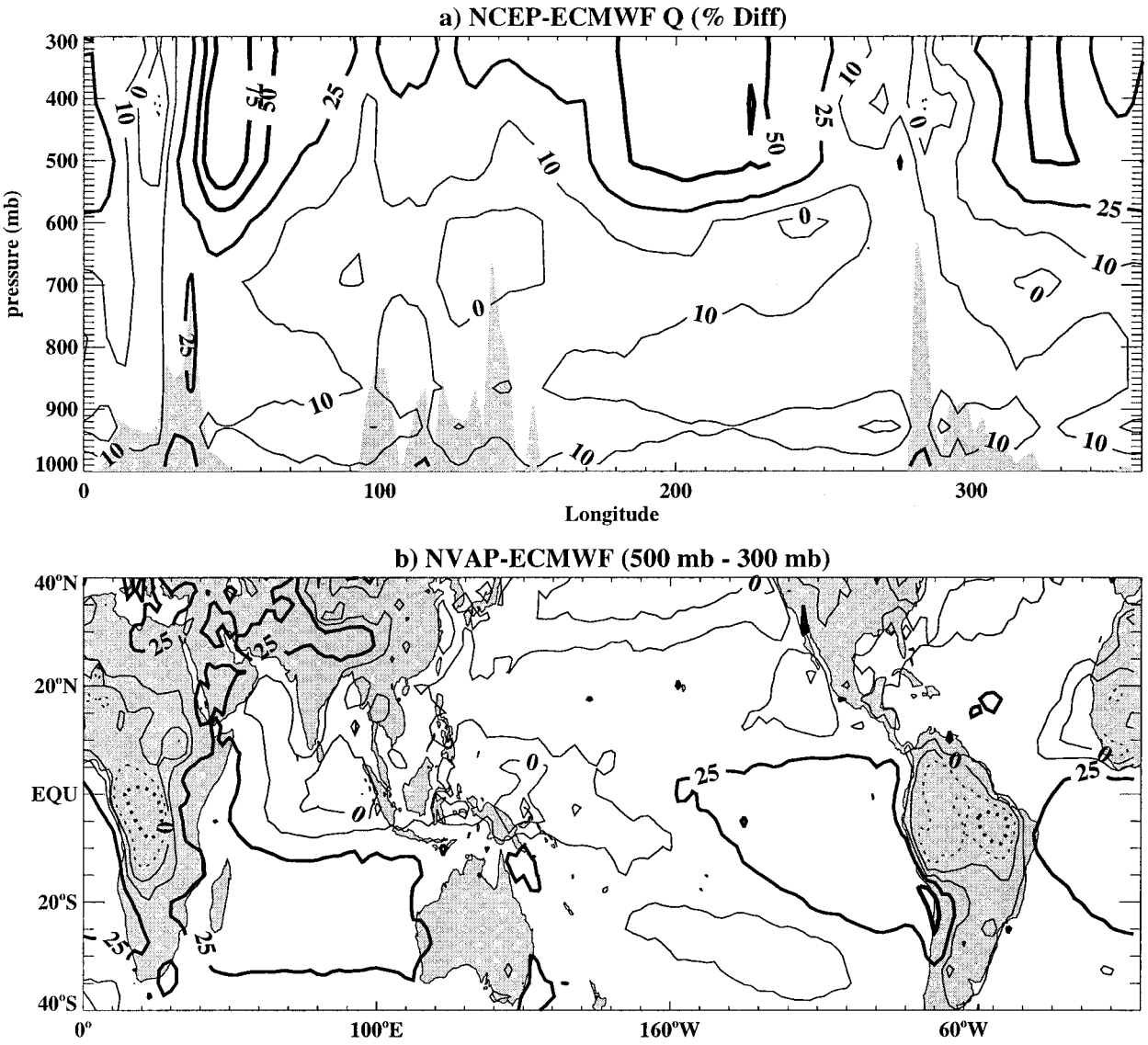

FIG. 1. Humidity differences between (a) the ECMWF and NECP–NCAR reanalysis averaged across 5°S–5°N and (b) the ECMWF reanalysis and NVAP retrievals from 500 to 300 mb.

balance is therefore constructed here. Aspects of the radiative model and the methodology used are discussed in section 2. The sensitivity of the mean surface and TOA radiative balance to the distribution of total columnar water vapor is assessed in section 3. The linearity of sensitivities are also discussed. In section 4, the sensitivity of the atmosphere's radiative budget to the vertical distribution of water vapor is then assessed.

2. Radiative transfer: Model and methodology

The radiative transfer calculation is performed using a 52-level version of the Community Climate Model, version 3, (CCM3; Kiehl et al. 1996) radiative transfer code from NCAR and is based on the modeling technique developed by Bergman and Hendon (1998). The model is a plane-parallel model that divides the solar spectrum into 18 intervals chosen to resolve important absorption lines in water vapor and other trace gas spectra. The delta-Eddington approximation is used to calculate fluxes at the surface and the TOA. Both the longwave and shortwave radiative properties of clouds are parameterized based on the cloud percent and cloud liquid water in each layer. Constant aerosol concentrations are included.[1] Calculations of water vapor sensitivity using an alternate radiative model with more detailed representation of the longwave spectrum and a larger number of trace gases (Icano et al. 2000) compare

[1] A more complete description of the radiative model is available from Briegleb (1992).

TABLE 1. Source and sampling characteristics of fields used as inputs to the radiative analysis.

Field	Source	Resolution	
		Spatial	Temporal
Air temperature	ECMWF	2.5°	6-h
Humidity	ECMWF	2.5°	6-h
Clouds	ISCCP	2.5°	3-h
SST	Reynolds (Reynolds and Smith 1994)	1°	Weekly

within 15% of the sensitivities produced by the CCM3 code.

The model input data, which are summarized in Table 1, include surface properties and vertical profiles of temperature, cloud fraction, cloud water content, water vapor, and ozone. Cloud fields from the International Satellite Cloud Climatology Project (ISCCP; Rossow and Schiffer 1991) C2 dataset are used in conjunction with atmospheric temperature and humidity fields from the ECMWF analyses. Cloud profiles are adjusted assuming a random overlap of various cloud types. The model is run using monthly mean atmospheric conditions such as temperature and humidity that sample the diurnal cycle at 3-h intervals. Fields are then interpolated to 1-h intervals across which the model is run. The method has been validated by Bergman and Hendon (1998) who show that tropical mean disagreement at the TOA is near 10 W m^{-2} for longwave and 20 W m^{-2} for shortwave fluxes. Figure 2 shows the model-produced out-

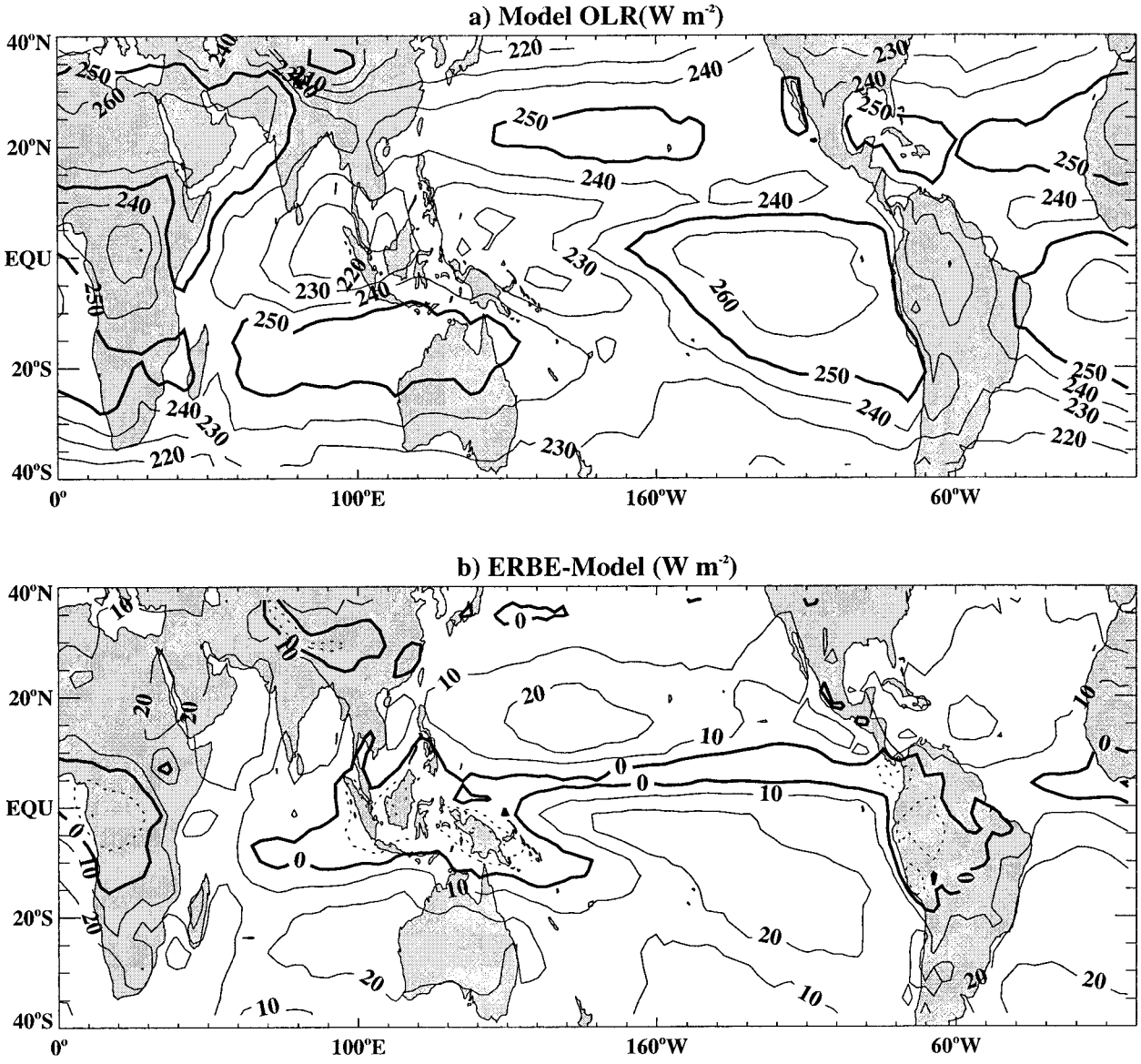

FIG. 2. (a) All-sky mean OLR simulated by the model and (b) its difference from ERBE observations.

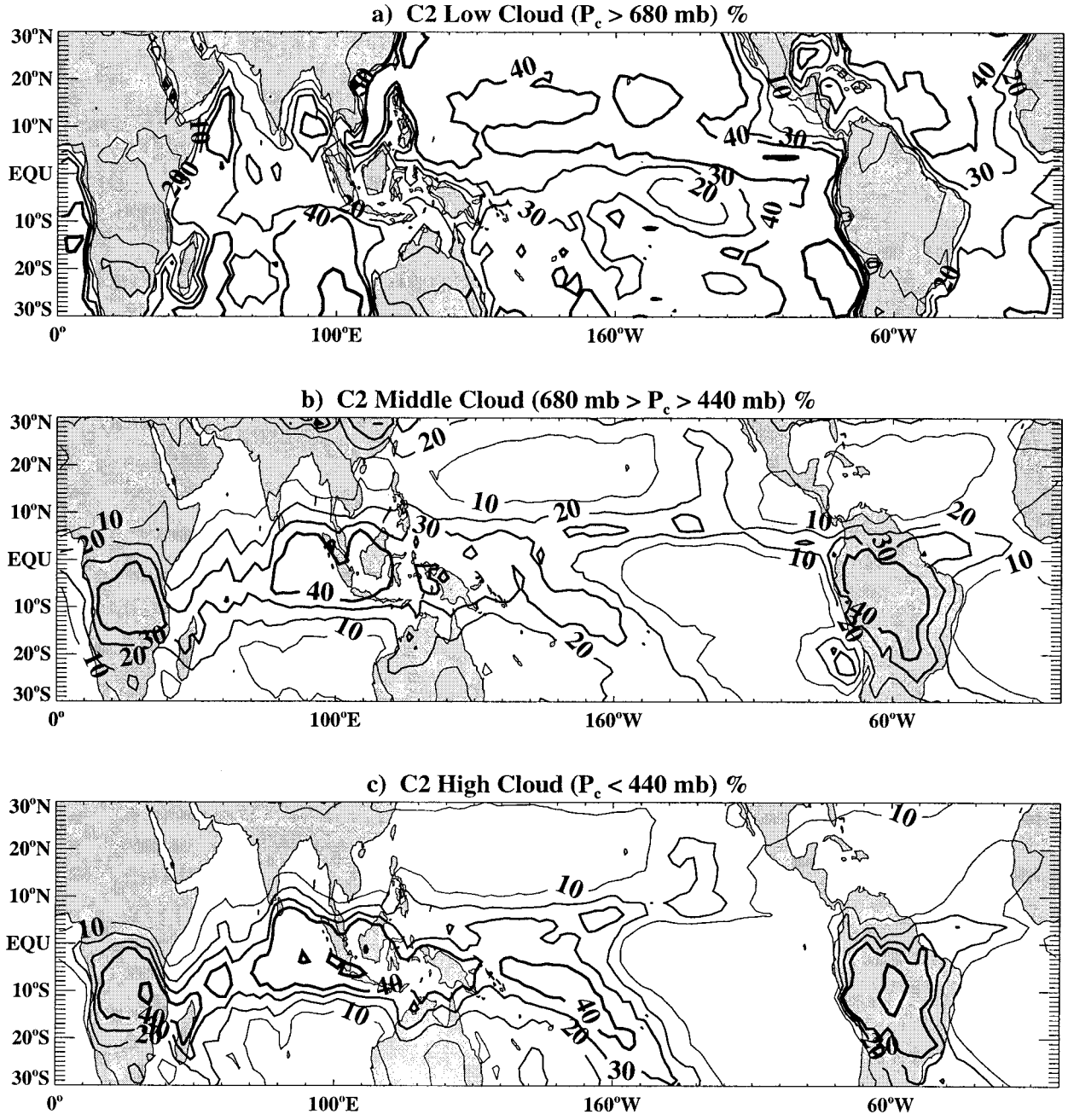

FIG. 3. ISCCP C2 mean cloud percent for (a) low, (b) middle, and (c) high clouds.

going longwave radiation (OLR) field and the difference between it and observations from the Earth Radiation Budget Experiment (ERBE; Barkstrom 1984). Many features in the satellites' mean OLR distribution are characterized well by the model, including the location and opacity of the subtropical dry zones and the deep convective regions of the western Pacific, Africa, and South America. Rms difference between ERBE and model OLR fields is about 12 W m^{-2}. The model's OLR is slightly too large in the deep convective regions and too small in the subtropical domains, suggesting that the model's greenhouse effect for water vapor may be slightly too weak and for clouds may be too strong. Nonetheless, the difference between the model and ERBE is not significantly greater than differences between narrowband and broadband satellite products, which lie between 5 and 10 W m^{-2} across much of the Tropics (Barkstrom 1984).

As an understanding of the cloud field is useful in interpretting calculated sensitivities, the ISCCP C2 cloud distribution is first assessed. Figure 3 shows overlap-adjusted cloud percent through the Tropics for low,

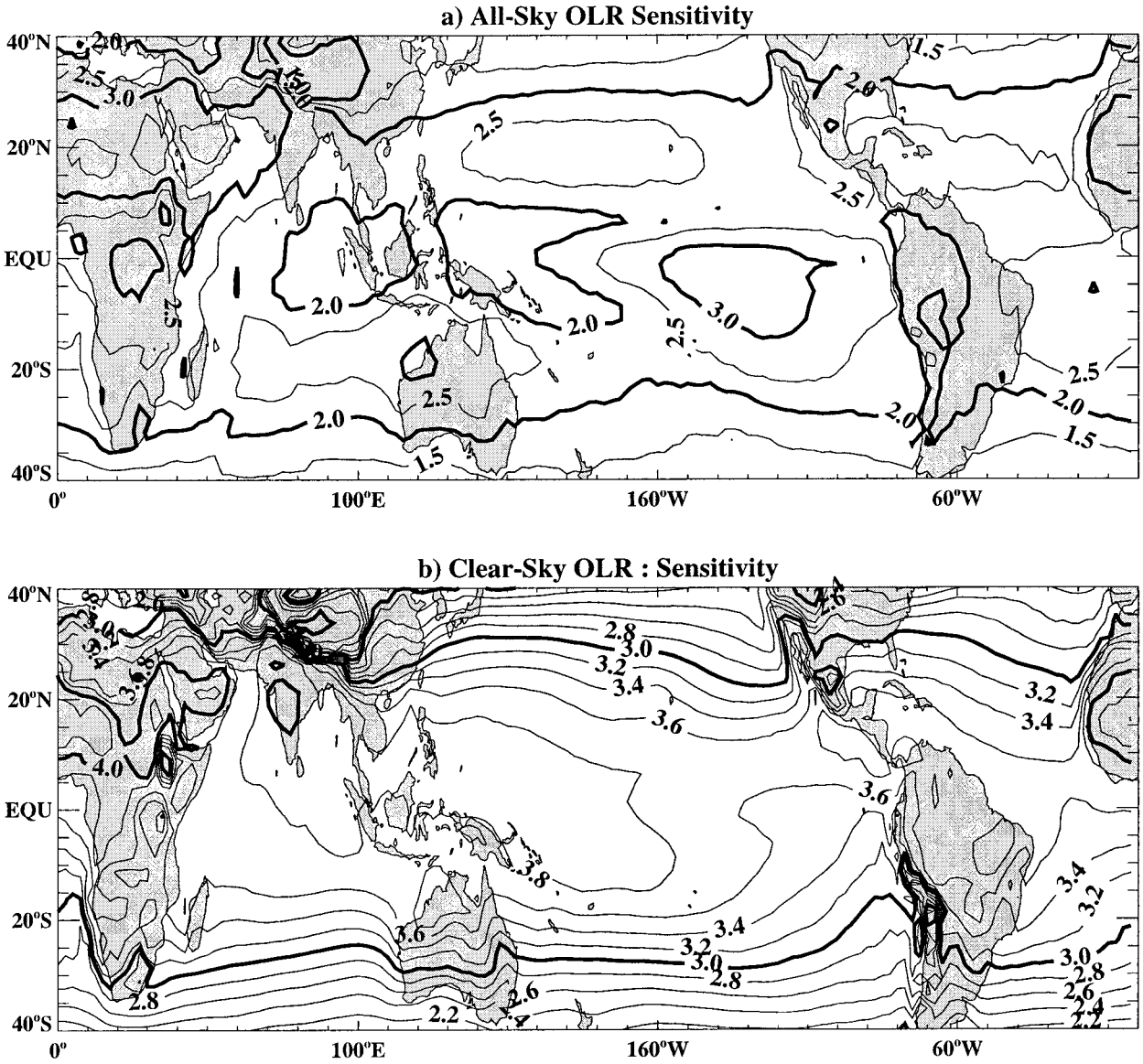

FIG. 4. OLR sesitivity to a 10% tropospheric drying for (a) all-sky and (b) clear-sky conditions.

medium, and high clouds. Low cloud is the predominant cloud type over the tropical oceans, with exceptionally high frequency in the subtropical eastern ocean basins (>50%). Mid- and upper-level clouds (Figs. 3b,c) experience a strong spatial coherence with the intertropical convergence zone (ITCZ). High clouds are nearly absent from the eastern Pacific Ocean and subtropical ocean.

3. Sensitivity of radiative fluxes to the distribution of water vapor

Figure 4 shows the increase in OLR due to a 10% reduction in tropospheric water vapor for all-sky and clear-sky conditions. Under all-sky conditions (Fig. 4a), peak sensitivity exists in the dry tropical and subtropical domains where OLR values are large (Fig. 2a), clouds are sparse (Fig. 3), and total greenhouse trapping is strongly influenced by water vapor. Measurement uncertainty in these arid regions is also particularly large (Fig. 1b). However, clear-sky sensitivity (Fig. 4b) is less in the eastern Pacific than in the western Pacific and the zonal gradient in sensitivity across the basin is therefore identified as a direct consequence of the cloud distribution. Sensitivity without clouds in the deep convective regions is approximately twice as large as with clouds (+2.0 vs 4.0 W m^{-2}) while, in subsident regions, it is only modestly impacted (+3.2 vs 3.6 W m^{-2}). Confidence in these findings is bolstered by the calculated tropical mean clear-sky sensitivity of 3.2 W m^{-2}, which agrees to within 10% of that found by Shine and Sinha (1991) under clear-sky conditions using a higher-resolution narrowband radiative transfer model.

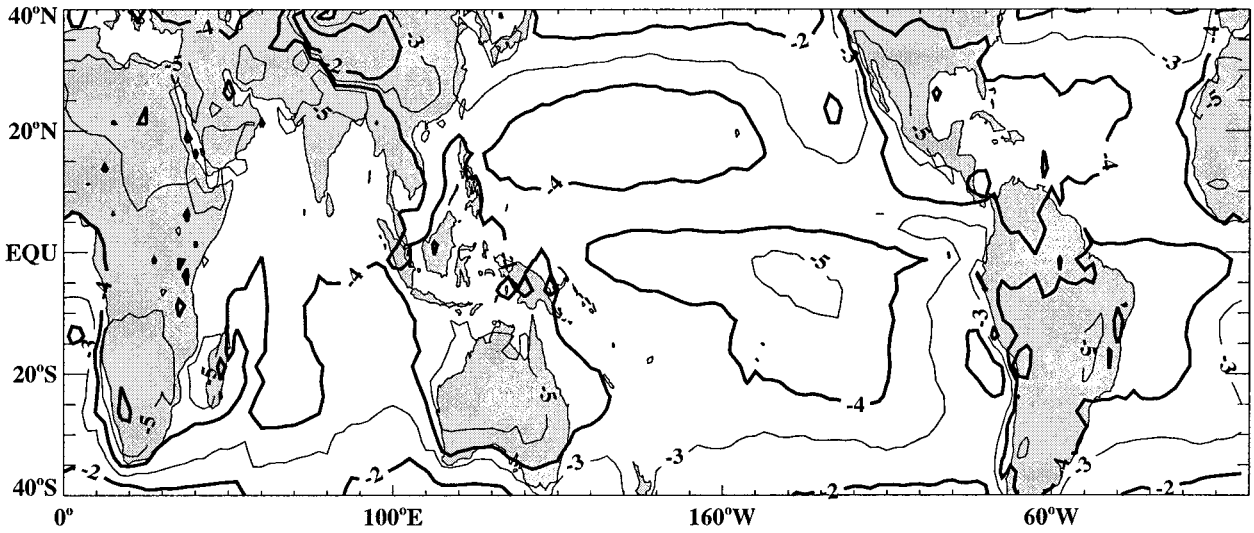

FIG. 5. Downwelling longwave flux sensitivity to a 10% reduction in water for all-sky conditions.

Surface downwelling longwave flux is composed primarily of emissions from the moist boundary layer and lowest cloud level, and its simulation therefore requires a correct depiction of cloud base, for which global observations are not available. Here cloud base is inferred from the convective condensation level of ECMWF temperature and humidity fields. Simulation of downwelling flux under this assumption yields a realistic downwelling longwave flux of 430 W m^{-2} in the moist convective regions of the ITCZ, western Pacific Ocean, and deep continental convective regions, and 400–420 W m^{-2} in the subtropical dry zones and eastern Pacific Ocean (not shown). Figure 5 shows the sensitivity of downwelling long flux to a 10% drying under all-sky and clear-sky conditions. All-sky sensitivity varies regionally, ranging from near 5 W m^{-2} in the central Pacific Ocean and subtropical ocean to 4 W m^{-2} in the deep convective zones. Near the western coasts of South and Central America, sensitivity achieves a tropical minimum of 2 W m^{-2} due to a dense low cloud field (Fig. 3a) that obscures the longwave impact of moisture in the free troposphere. In the western Pacific, sensitivity is low because of a dense low- and midcloud field.

The linearity of sensitivities is shown in Table 2, where both the tropical mean sensitivity and its deviation from a linear extrapolation of the 10% drying perturbation are indicated. OLR sensitivity is approximately linear, differing with an extrapolation of the 10% drying case by only 12%. Somewhat less linear is the sensitivity of the surface downwelling longwave flux that decreases as the environment dries. Nonetheless, its sensitivity is within 30% of that expected from a linear extrapolation from the 10% drying case. Both total columnar longwave heating and net surface radiation exhibit strong nonlinearity as a 30% moistening deviates by up to 50% from that expected from extrapolation of the 10% drying case. The greatest nonlinearity is found in the surface shortwave flux; however, the absolute magnitude of the flux's sensitivity is small as compared with other sensitivities (e.g., Arkin 1999).

4. Sensitivity to the vertical distribution of water vapor

Lindzen (1990) and Sun and Lindzen (1993a) identify the importance of radiative sensitivity to height-dependent changes in water vapor due to the potential role of convective processes in modifying the water vapor distribution. Here the studies of Shine and Sinha (1991) and Schneider et al. (1999) are extended by including observed clouds and assessing vertically varying water vapor changes that are characteristic of both natural variability and measurement uncertainty. Sensitivity is assessed for perturbations whose magnitudes vary with

TABLE 2. Difference between tropical mean flux perturbations for 10% and 30% tropospheric drying and moistening. Also shown is the percentage deviation of the calculated sensitivity from a linear extrapolation of a 10% drying.

Flux	−30%	−10%	10%	30%
Net OLR	+6.98 (+7%)	+2.17	−2.04 (−6%)	−5.76 (−12%)
Surface downwelling shortwave	+3.12 (+92%)	+0.54	−1.24 (+130%)	−2.37 (+46%)
Surface downwelling longwave	−13.13 (−16%)	−3.76	+3.21 (−14%)	+8.23 (−27%)
Net columnar longwave heating	+6.15 (+28%)	+1.59	−1.17 (−26%)	−2.47 (−48%)
Net surface radiation	−10.01 (4%)	−3.22	+1.97 (−38%)	+5.86 (−39%)

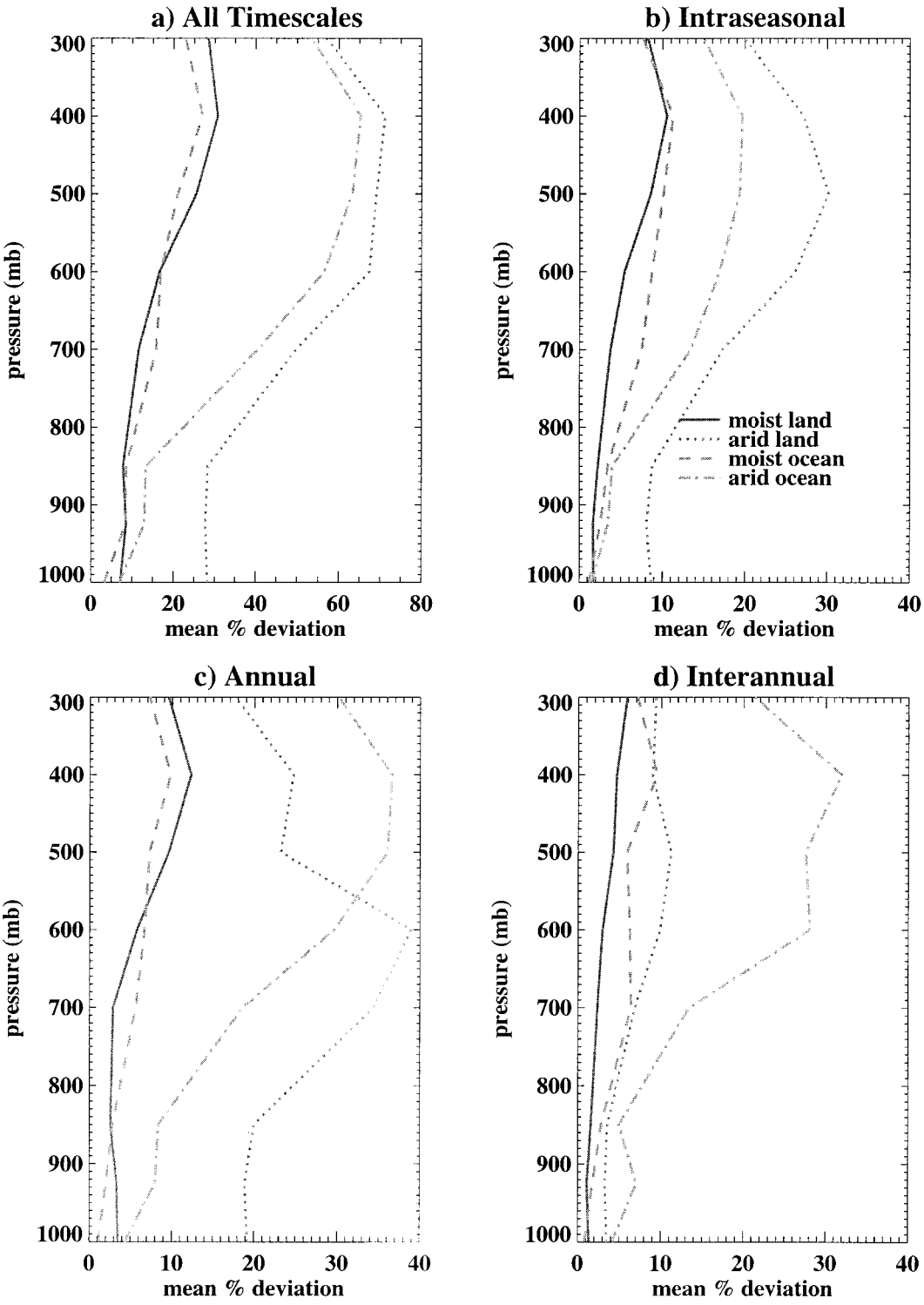

FIG. 6. Mean magnitude of variations in water vapor amounts by level as a percentage of the long-term mean from the NCEP–NCAR reanalysis for (a) unfiltered, (b) intraseasonal, (c) seasonal, and (d) interannual variations.

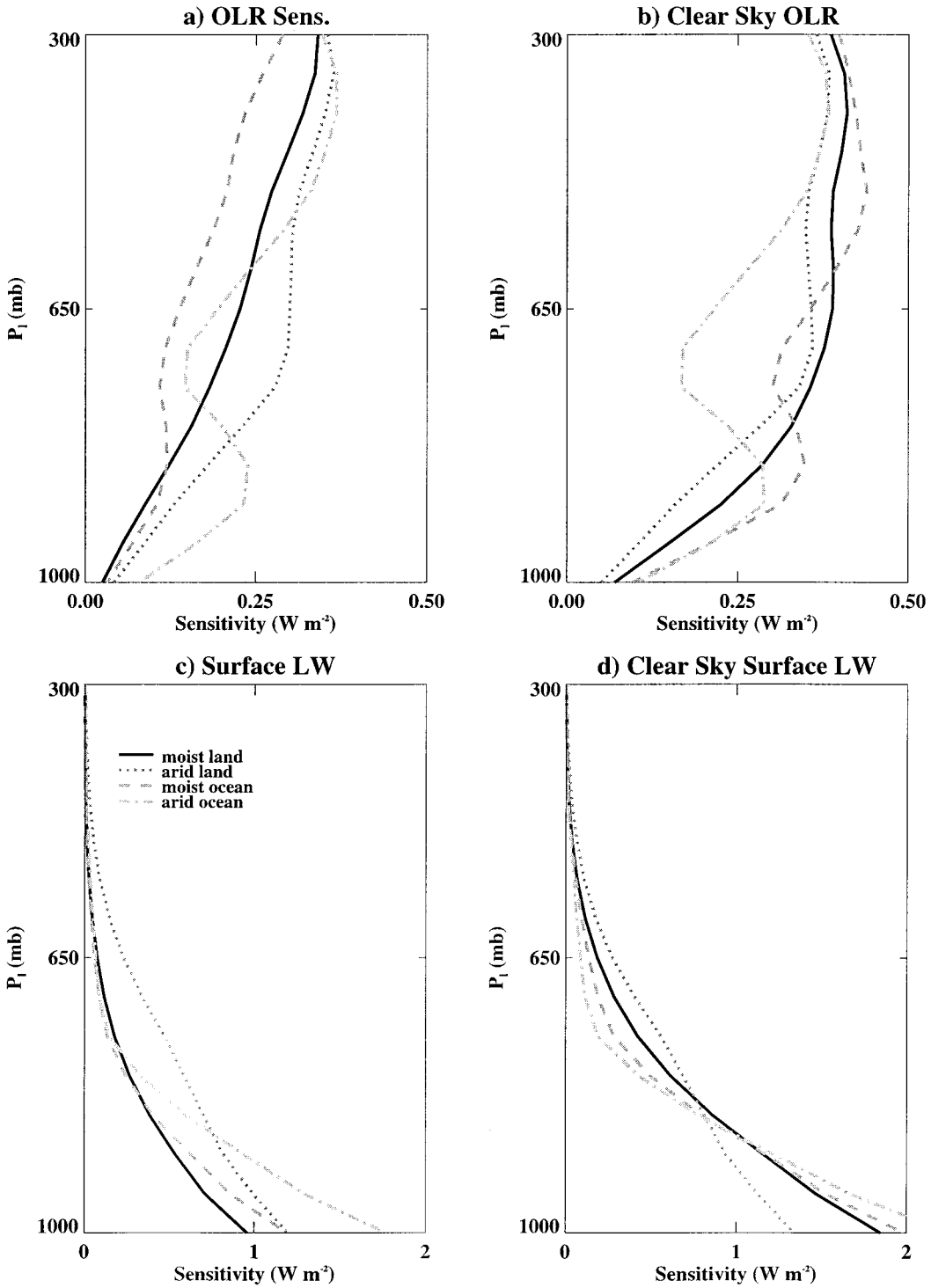

FIG. 7. Sensitivity of longwave fluxes to perturbations scaled linearly from 10% near the surface to 50% at 300 mb at the TOA and surface for (left) all-sky and (right) clear-sky conditions.

height in order to represent better the impact of uncertainty and variability in the moisture field (Figs. 1 and 2). The sites over which sensitivity will be assessed are equatorial (0°, 20°E) and northern (20°N, 20°E) Africa, and the equatorial western (0°, 155°E) and eastern Pacific Oceans (0°, 130°W). The sites represent moist and arid conditions over land and ocean, respectively.

Figure 6 shows the mean percentage departures from the long-term climatology of specific humidity at the four study sites as reported by the NCEP–NCAR re-

analysis dataset as a function of height and timescale. Unfiltered variations show peak variability near 400 mb for all sites with magnitudes approaching 30% for the moist regions and 60% for arid regions. Variability in the lower troposphere is modest (~10%) for all sites except over the arid land site. Variations on intraseasonal (Fig. 6b), seasonal (Fig. 6c), and interannual (Fig. 6d) timescales assessed from NCEP–NCAR reanalysis data also show that fluctuations in the mid- and upper troposphere are generally more than twice as large as at the surface. Thus the vertical structure of variability in the water vapor distribution coarsely resembles its uncertainty (Figs. 1 and 2).

Figure 7 displays the sensitivity of fluxes at the surface and TOA to specific humidity variations that have been scaled linearly from 10% at 1000 mb to 50% at 300 mb in order to represent better the variability and uncertainty in the water vapor field. When perturbations are allowed to vary with height, the TOA longwave budget for all four regions is considerably more sensitive to water vapor in the mid- and upper troposphere under both all-sky (Fig. 7a) and clear-sky (Fig. 7b) conditions. As with the sensitivity to a 10% perturbation, greatest all-sky sensitivity is realized for the arid land and ocean sites. Peak sensitivity is near 400 mb and is somewhat deeper in the troposphere than identified by Schneider et al. (1999) and much deeper than found by Shine and Sinha (1991). A correct depiction of both upper-tropospheric moisture and clouds is necessary to assess TOA radiative sensitivities realistically. Surface radiative fluxes are most sensitive to perturbations in the lower troposphere (>700 mb), however, with rapid reductions in sensitivity with height through much of the free troposphere. Lower-tropospheric moisture is therefore key to the surface energy balance and coupled simulations of the ocean and atmosphere. As surface flux sensitivity is roughly 2 to 3 times larger at the surface than at the TOA (Table 2), the sensitivity of longwave divergence within the troposphere is also dominated by lower-tropospheric variations.

5. Conclusions

Differences in the water vapor distribution among available datasets demonstrate that large uncertainties exist in assessment of the mean distribution. A numeric study of radiative sensitivities to perturbations in water vapor has been carried out using realistic clouds. At both the TOA and the surface, net radiative sensitivity is dominated by the longwave spectrum and is largest in the dry zones of the subtropics and eastern Pacific Ocean where measurement uncertainty is also large. The results underscore the important role the arid tropical and subtropical regions play in the climate's radiative balance.

A strong relationship between lateral gradients in sensitivity and clouds is identified. In regions of frequent high clouds, sensitivity at TOA is significantly reduced from the cloud-free and low-cloud environments. Similarly, surface radiative fluxes in regions dominated by frequent low clouds are less sensitive than in regions where low clouds are rare. Longwave sensitivity is more than 2 times as large at the surface than at TOA and is therefore the dominant component of total columnar heating sensitivity. At both the surface and TOA, solar flux sensitivities are of opposite sign and are substantially reduced from those in the longwave. Sensitivity of TOA fluxes to natural variability and measurement uncertainty is substantially greater in the mid- and upper troposphere than in its lower layers. In contrast, surface fluxes are more strongly impacted by the lower troposphere, and low-level variations are therefore critical for coupled simulations.

A principal caveat of the current findings regards the assumption of a fixed cloud field. Indeed, in nature the cloud field is strongly tied to the distribution of water vapor, and a complete assessment of the radiative importance of water vapor will include the consequent cloud response. The lack of an adequate means by which to characterize this response has led to the assumption of a fixed cloud field in both the current study and model assessments (e.g., Schneider et al. 1999). A comprehensive assessment of the response of the cloud field will be a valuable asset for further understanding climate's sensitivity to water vapor.

Acknowledgments. This work was completed while Dr. Fasullo was at the NOAA Climate Diagnostics Center in Boulder, Colorado, and was funded by NOAA's PACS Program (NOAA Grant NA06GP0022). The authors thank Dr. J. Bergman for providing the radiation code and methodology for integrating ISCCP observations in the radiative scheme. The NCEP–NCAR reanalysis data were provided by the Climate Diagnostics Center.

REFERENCES

Arking, A., 1990: The influence of clouds and water vapor on atmospheric absorption. *Geophys. Res. Lett.,* **26,** 2729–2732.

Barkstrom, B. R., 1984: The Earth Radiation Budget Experiment (ERBE). *Bull. Amer. Meteor. Soc.,* **65,** 1170–85.

Bergman, J. W., and H. H. Hendon, 1998: Calculating monthly radiative fluxes and heating rates from monthly cloud observations. *J. Atmos. Sci.,* **55,** 3471–3492.

Betts, A. K., 1990: Greenhouse warming and the tropical water vapor budget. *Bull. Amer. Meteor. Soc.,* **71,** 1465–1467.

Briegleb, B. P., 1992: Delta-Eddington approximation for solar radiation in the NCAR Community Climate Model. *J. Geophys. Res.,* **97,** 7603–7612.

Elliot, W. P., and D. J. Gaffen, 1991: On the utility of radiosonde humidity archives for climate studies. *Bull. Amer. Meteor. Soc.,* **72,** 1507–1520.

Gibson, J. K., P. Kallberg, S. Uppala, A. Hernandez, A. Nomura, and E. Serrano, 1997: ECMWF Reanalysis Project Rep. Ser. 1. ECMWF, Shinfield Park, Reading, United Kingdom, 72 pp. [Available from ECMWF, Shinfield Park, Reading, RG2 9AX, United Kingdom.]

Iacono, M. J., E. J. Mlawer, S. A. Clough, and J.-J. Morcrette, 2000: Impact of an improved longwave radiation model, RRTM, on the energy budget and thermodynamic properties of the NCAR

Community Climate Model, CCM3. *J. Geophys. Res.,* **105,** 14 873–14 890.

Kalnay, E., and Coauthors, 1996: The NCEP/NCAR 40-Year Reanalysis Project. *Bull. Amer. Meteor. Soc.,* **77,** 437–471.

Kiehl, J. T., J. J. Hack, G. B. Bonan, B. A. Boville, B. P. Briegleb, D. L. Williamson, and P. J. Rasch, 1996: Description of the NCAR Community Climate Model (CCM3). Tech. Note NCAR/TN420+STR, NCAR, 152 pp. [Available from University Corporation for Atmospheric Research, P. O. Box 3000, Boulder, CO 80307.]

Lindzen, R., 1990: Some coolness concerning global warming. *Bull. Amer. Meteor. Soc.*,**71,** 288-299.

Manabe, S., and R. T. Wetherald, 1967: Thermal equilibrium of the atmosphere with a given distribution of relative humidity. *J. Atmos. Sci.,* **24,** 241–259.

Randel, D. L., T. H. Vonder Haar, M. A. Ringerud, G. L. Stephens, T. J. Greenwald, and C. L. Combs, 1996: A new global water vapor dataset. *Bull. Amer. Meteor. Soc.,* **77,** 1233–1246.

Reynolds, R. W., and T. M. Smith, 1994: Improved global sea surface temperature analyses using optimum interpolation. *J. Climate* **7,** 929–948.

Rind, D., E.-W. Chow, W. Cho, J. Larsen, S. Oltmons, J. Lerner, M. P. McCormick, and L. McMaster, 1991: Positive water vapour feedback in climate models confirmed by satellite data. *Nature,* **349,** 500–503.

Rossow, W. B., and R. A. Schiffer, 1991: ISCCP cloud data products. *Bull. Amer. Meteor. Soc.,* **72,** 2–20.

Schneider, E. K., B. P. Kirtman, and R. S. Lindzen, 1999: Tropospheric water vapor and climate sensitivity. *J. Atmos. Sci.,* **56,** 1649–1658.

Shine, K. P., and A. Sinha, 1991: Sensitivity of the earth's climate to height dependent changes in the water vapor mixing ratio. *Nature,* **354,** 382–384.

Sun, D.-Z., and R. S. Lindzen, 1993a: Distribution of tropical tropospheric water vapor. *J. Atmos. Sci.,* **50,** 1643–1660.

——, and ——, 1993b: Water vapor feedback and the ice age snowline record. *Ann. Geophys.,* **11,** 204–215.

——, and A. H. Oort, 1995: Humidity–temperature relationships in the tropical troposphere. *J. Climate,* **8,** 1974–1987.

——, and I. M. Held, 1996: A comparison of modeled and observed relationships between interannual variations of water vapor and temperature. *J. Climate,* **9,** 665–675.

Zipser, E. J., and R. H. Johnson, 1998: Systematic errors in radiosonde humidities: A global problem? Preprints, *10th Symp. on Meteorological Observations and Instrumentation,* Phoenix, AZ, Amer. Meteor. Soc., 72–73.